Negative refraction and subwavelength imaging of a photonic-crystal slab for the frequencies in the third band

Shuai Feng (冯 帅)[1*], Cheng Ren (任 承)[2], Degang Xu (徐德刚)[3], and Yiquan Wang (王义全)[1]

[1]*Academy of Science, Minzu University of China, Beijing 100081, China*

[2]*School of Opto-Electronic Information Science and Technology, Yantai University, Yantai 264005, China*

[3]*College of Precision Instruments and Opto-Electronic Engineering, Tianjin University, Key Laboratory of Opto-Electronic Information Science and Technology, Ministry of Education, Tianjin 300072, China*

[*]*E-mail: fengshuai75@163.com*

Received December 22, 2008

Negative refraction and subwavelength imaging properties of a two-dimensional (2D) photonic crystal (PC) slab are studied by the finite-difference time-domain method. The PC consists of a triangular lattice of air holes immersed in a dielectric. For a certain frequency range in the third photonic band, the directions of the group velocities and the phase velocities can be opposite, so the PC can work as a kind of negative refractive-index material. The light radiated from a point source can form a subwavelength image spot through the PC slab. Negative refraction and an effective refractive index of the PC slab $n = -1$ can be achieved for the incident wave with its incident angle within a certain range.

OCIS codes: 260.1180, 250.0250, 160.4670.

doi: 10.3788/COL20090709.0849.

Negative refractive-index materials (NIMs), whose permeability and permittivity are simultaneously negative, have attracted much attention and a great deal of interest since their experimental realization several years ago[1−5]. A NIM slab can amplify the evanescent wave components involved in the radiation from a point source and accomplish excellent retrieval of the fine information, which is necessary for the formation of a high-quality image. Negative refraction can be achieved in some two-dimensional (2D) and three-dimensional (3D) photonic crystals (PCs)[6−18]. Luo *et al*. showed that subwavelength imaging can be achieved at the lowest band of 2D square-lattice PCs and at a wavelength four times larger than the lattice constant[6]. Zhang showed that a non-near-field image can be achieved in the second band of the 2D triangular-lattice PC slab consisting of coated cylinders immersed in the air[7]. Feng *et al*. showed that subwavelength imaging can be achieved in the lowest TM-polarized bands of both the 2D square-lattice and triangular-lattice metallic PC slabs[8,9]. Up to now, most discussions are concerned about the negative refraction and imaging properties of the frequencies at the low bands of the square-lattice and triangular-lattice PC slabs. Now exploring the new structure of PC slab through which negative refraction occurs for the frequencies in higher bands attracts people's attention. In this letter, we show that negative refraction and imaging can be achieved in the third TE-polarized band of a 2D triangular-lattice PC slab consisting of air holes immersed in a dielectric.

A 2D PC slab consisting of a triangular lattice of air holes immersed in a dielectric $\varepsilon = 18$ (that of Ge at 1.55 μm) is considered in this letter. The radius of the air holes is $r = 0.35a$, where a is the lattice constant of the PC. The study of the negative refraction and imaging effect of a PC slab usually starts from the investigation of the photonic band structures and the equifrequency-surface (EFS) contours. We employ the plane-wave expansion method to calculate the band structures and the EFS contours of the above PC. In order to obtain a high enough resolution of the fine structure of the curve, 961 plane waves are adopted and more than 10000 Bloch-wave vectors within the first Brillouin zone (BZ) of the triangular lattice are used for constructing the EFS contour in all the calculations. The calculated TE-polarized band structures along the several high-symmetric lines in the first BZ are shown in Fig. 1. We see that a complete band gap occurs between the first and second bands and lies at 0.181−0.281 (in units of $2\pi c/a$, where c is the velocity of light in vacuum), and the third band spans from 0.293 to 0.396. The calculated EFS contours of the frequencies in the third photonic band are shown in Fig. 2. It can be seen that some EFS contours such as 0.36 and 0.38 are

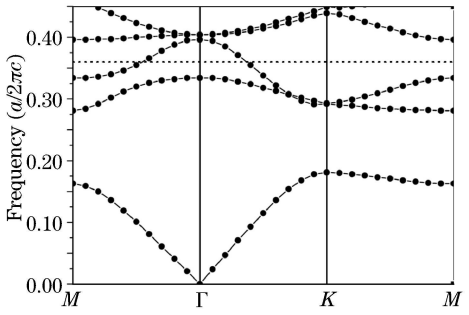

Fig. 1. TE-polarized photonic band structures of the PC consisting of a triangular lattice of air holes in a dielectric with $\varepsilon = 18$. The radius of the air holes is r=0.35a.

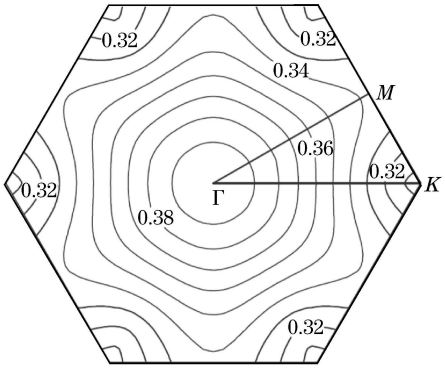

Fig. 2. Several EFS contours in the third TE-polarized photonic band of the PC depicted in Fig. 1.

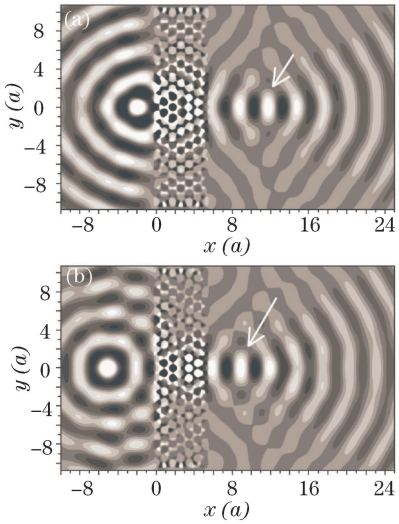

Fig. 3. Field patterns of the EM waves radiated from a point source through the PC slab. The rectangular PC slab is 41 layers wide and 9 layers thick. The slab surface normal is along the ΓK direction. The point source resonating at frequency 0.36 is placed at $y = 0$, and (a) $x = -2a$, (b) $x = -5a$, respectively. The arrows point at the positions of the image spots.

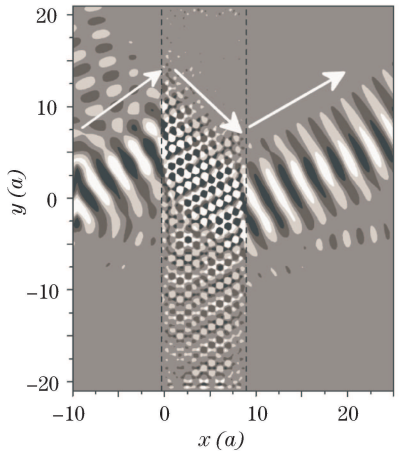

Fig. 4. Negative refraction of an incident light beam through the PC slab. The frequency of the incident light beam is $\omega = 0.36$. The PC slab with the surface normal pointing along the ΓK direction is 11 layers thick, which is shown by two dashed lines. The three arrows point to the transmission directions of the light beam inside and outside the PC slab.

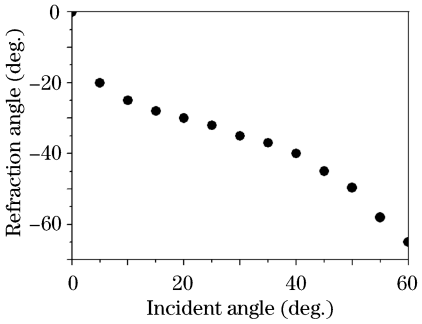

Fig. 5. Refraction angle versus incident angle at the frequency $\omega = 0.36$ for the TE-polarized wave.

almost round, indicating that the PC can be regarded as an equivalent isotropic medium at these incident frequencies. The frequencies increase inwards, that is to say, the group velocities are opposite to the phase velocities, which means that the transmitting features of the electromagnetic (EM) wave in the PC are the negative refraction behavior.

Now we employ the finite-difference time-domain method[19,20] with a boundary treatment of perfectly matched layers to visualize the propagation of EM waves through the PC slab. At first, the rectangular PC slab is constructed to be 41 layers wide and 9 layers thick with the surface normal parallel to the ΓK direction. The distances from the left and right slab surfaces to the center of the adjacent air holes are $0.35a$. Thus the thickness of the PC slab is $5.4a$. The center of the air holes in the first layer is located at $x = 0$, and the slab is symmetric with respect to $y = 0$. A point source of continuous wave resonating at the frequency $\omega = 0.36$ is placed at the left side of the PC slab.

When the location of the point source is placed at $x = -2a$, $y = 0$, the calculated field patterns of the EM wave propagation radiated from the point source are shown in Fig. 3(a). It can be seen that the EM wave emitted from the point source transmits through the PC slab and forms an image spot in the opposite side of the slab. The image spot is located at a distance of $4.5a$ from the right surface of the slab. The width of the image spot (full size at half maximum in the lateral direction) is about $1.9a$, corresponding to 0.684λ. Figure 3(b) shows the calculated field distribution of the EM wave propagation when the location of the point source is changed to $x = -5a$ and $y = 0$. It can be seen that an apparent image spot is formed at a distance of $1.5a$ from the right side of the PC slab. The width of the image spot is also about $1.9a$, corresponding to 0.684λ.

When a light beam of frequency $\omega = 0.36$ is incident from air to the left surface of the PC slab, which is 11 layers thick with the surface normal pointing at the ΓK direction, it can be seen from Fig. 4 that the refractive light beams within and outside the PC slab travel on the path of negative refraction. The incident angle is 45° and the two refractive angles are both about 45°. We can see that negative refraction occurs and an effective refractive index $n = -1$ is obtained. Figure 5 shows the angles of refraction changed with the incident angles, from which we can see that effective index is almost equal to -1 at the incident angles around 45°. The EFS contour of the frequency 0.36 has a hexagonal symmetry, not a perfect

circle, which causes that the effective index deviates from −1 when the incident angle moves away from 45°.

In conclusion, we have studied the negative refraction and focusing properties of the 2D triangular-lattice PC slabs consisting of air holes in a dielectric. An image spot can be formed in the third TE-polarized photonic band and negative refraction of the incident light beams through the PC slab is also observed. These simulation results may bring some interests of engineering involving the negative refraction and imaging properties of PC slab lens, and accelerate the actual utilization of the negative refraction and focusing properties of PC slab lens.

This work was supported by the National Key Basic Research Special Foundation of China (Nos. 2006CB921702 and 2007CB310403), the National Natural Science Foundation of China (Nos. 10674185 and 10801017), and the Youth Foundation of Minzu University of China.

References

1. J. B. Pendry, Phys. Rev. Lett. **85,** 3966 (2000).
2. V. G. Veselago, Sov. Phys. Usp. **10,** 509 (1968).
3. J. Li, L. Zhou, C. T. Chan, and P. Sheng, Phys. Rev. Lett. **90,** 083901 (2003).
4. D. R. Smith and D. Schurig, Phys. Rev. Lett. **90,** 077405 (2003).
5. R. A. Shelby, D. R. Smith, and S. Schultz, Science **292,** 77 (2001).
6. C. Luo, S. G. Johnson, J. D. Joannopoulos, and J. B. Pendry, Phys. Rev. B **65,** 201104(R) (2002).
7. X. Zhang, Phys. Rev. B **70,** 195110 (2004).
8. S. Feng, Z.-Y. Li, Z.-F. Feng, B.-Y. Cheng, and D.-Z. Zhang. Appl. Phys. Lett. **88,** 031104 (2006).
9. S. Feng, M. Sun, C. Ren, K. Ren, Z.-F. Feng, Z.-Y. Li, B.-Y. Cheng, and D.-Z. Zhang, Chin. Phys. Lett. **23,** 994 (2006).
10. L. Feng, X.-P. Liu, M.-H. Lu, Y.-B. Chen, Y.-F. Chen, Y.-W. Mao, J. Zi, Y.-Y. Zhu, S.-N. Zhu, and N.-B. Ming, Phys. Rev. Lett. **96,** 014301 (2006).
11. J. Li, M.-H. Lu, T. Fan, X.-K. Liu, L. Feng, Y.-F. Tang, and Y.-F. Chen, J. Appl. Phys. **102,** 073538 (2007).
12. Z.-Y. Li and L.-L. Lin, Phys. Rev. B **68,** 245110 (2003).
13. S. Feng, Z.-Y. Li, Z.-F. Feng, B.-Y. Cheng, and D.-Z. Zhang, Phys. Rev. B **72,** 075101 (2005).
14. C. Qiu, X. Zhang, and Z. Liu, Phys. Rev. B. **71,** 054302 (2005).
15. Y.-T. Fang and T.-G. Shen, Chin. Phys. Lett. **22,** 949 (2005).
16. Y. Fang and Z. Ouyang, Chin. Opt. Lett. **6,** 57 (2008).
17. S. He, Z. Ruan, L. Chen, and J. Shen, Phys. Rev. B **70,** 115113 (2004).
18. X. Li, K. Xie, and H. Jiang, Chin. Opt. Lett. **6,** 130 (2008).
19. K. S. Yee, IEEE Trans. Antenn. Propag. **14,** 302 (1966).
20. J.-P. Berenger, J. Comput. Phys. **127,** 363 (1996).